Conformational Changes of an Hsp70 Molecular Chaperone Induced by Nucleotides, Polypeptides, and *N*-Ethylmaleimide†

William J. Chirico,*,‡ Micheline L. Markey,§ and Anthony L. Fink§

Department of Anatomy and Cell Biology, State University of New York Health Science Center at Brooklyn, Brooklyn, New York 11203, and Department of Chemistry and Biochemistry, University of California, Santa Cruz, California 95064

Received March 17, 1998; Revised Manuscript Received August 3, 1998

ABSTRACT: Hsp70 molecular chaperones are highly conserved ATPases that guide the folding and assembly of proteins in many cellular pathways. They use the energy of ATP binding and hydrolysis to regulate their interactions with hydrophobic regions of unfolded proteins. The activities and the conformations of the N-terminal nucleotide- and C-terminal polypeptide-binding domains of Hsp70s are coupled. We recently reported that the sulfhydryl-modifying reagent *N*-ethylmaleimide (NEM) inactivates the yeast Hsp70 Ssa1p by reacting with its three cysteine residues which are located in the nucleotide-binding domain. To further characterize conformational changes associated with interdomain coupling and to determine whether NEM alters Ssa1p's conformation, the structures of Ssa1p and NEM-modified Ssa1p (NEM-Ssa1p) were compared using a variety of biophysical techniques. Size exclusion chromatography revealed that NEM-Ssa1p is more oligomeric and more resistant to nucleotide- or polypeptide-dependent depolymerization than Ssa1p. Measurement of the thermal stability indicated that NEM modification has an effect very similar to that of binding of nucleotides to the unmodified protein. Circular dichroism demonstrated small differences in the secondary structure of Ssa1p and NEM-Ssa1p, and in their complexes with nucleotides. NEM modification increased the ANS fluorescence of Ssa1p and exposed numerous trypsin-sensitive sites in its nucleotide-binding domain. The intrinsic fluorescence of Ssa1p's only tryptophan residue, which is located in a C-terminal α-helical region adjacent to the polypeptide-binding cleft, was quenched in the presence of ATP, but not ADP. NEM modification altered nucleotide-dependent changes in the intrinsic fluorescence of Ssa1p. Together, these results demonstrate that NEM alters the conformation of Ssa1p and disrupts, but does not eliminate, interdomain communication. Furthermore, the results provide evidence for a model in which the polypeptide-binding cleft of Hsp70s is covered by an α-helical lid that is open in the presence of ATP, but closed in the presence of ADP.

Hsp70[1] molecular chaperones are ATPases that participate in many cellular pathways, including protein folding, translocation, and proteolysis (reviewed in ref *1*). They bind extended (*2*), hydrophobic regions of proteins (*3*−*5*), thereby preventing their irreversible aggregation (*6, 7*). Cooperative effects are observed in interactions of Hsp70s with nucleotides and polypeptides. For example, polypeptide substrates enhance ATPase activity 2−5-fold (*8*), and ADP stabilizes Hsp70−polypeptide complexes (*9*); on the other hand, ATP greatly accelerates binding and release of polypeptides (*10*). The interactions of nucleotides and polypeptides with Hsp70s are also regulated by protein modulators DnaJ, GrpE, and their homologues (*11*, *12*).

Hsp70 molecular chaperones are oligomeric proteins whose state of association is influenced by nucleotides and polypeptides (*13*−*18*). In the presence of ATP, Hsp70s are primarily monomeric, whereas in the presence of ADP, they exist as monomers, dimers, and larger oligomers (*13*, *14*). Analogous to ATP, polypeptides promote the monomerization of Hsp70s (*16*, *19*). Ydj1p, a DnaJ homologue of *Saccharomyces cerevisiae*, polymerizes Hsp70s in the presence of ATP (*13*).

The ATPase domain of Hsp70s is located in the 44 kDa N terminus, whereas the polypeptide-binding domain is located in the 27 kDa C terminus. The conformations of Hsp70s are influenced by nucleotides and polypeptide substrates (*17*, *20*−*26*). Nucleotide-free and ADP- and ATP-bound forms of Hsp70s have been described using fluorescent probes (*27*), intrinsic tryptophan fluorescence (*9*, *20*, *25*, *28*), and limited proteolysis (*20*−*22*). The conformation of the nucleotide-binding domain of the *S. cerevisiae* Hsp70 Ssa1p is altered by polypeptide binding to the C-terminal domain (*22*). Similarly, the conformation of its polypeptide-binding domain (*29*) is altered by the binding of nucleotides to the ATPase domain (*22*). Thus, the functions and the conformations of the two domains of Hsp70s are tightly regulated and coupled.

† Supported by a Grant-In-Aid from the American Heart Association New York City Affiliate to W.J.C.

* To whom correspondence should be addressed: Department of Anatomy and Cell Biology, SUNY-HSCB, Box 5, 450 Clarkson Ave., Brooklyn, NY 11203. Telephone: (718) 270-1308. Fax: (718) 270-3732. E-mail: wchirico@netmail.hscbklyn.edu.

‡ State University of New York Health Science Center at Brooklyn.

§ University of California.

[1] Abbreviations: Hsp70, 70 kDa heat shock protein; Hsc70, 70 kDa heat shock cognate protein; BiP, heavy chain binding protein; NEM, *N*-ethylmaleimide; NEM-Ssa1p, NEM-modified Ssa1p; DTT, dithiothreitol; ANS, 1-anilinonaphthalene-8-sulfonic acid; PAGE, polyacrylamide gel electrophoresis; CD, circular dichroism.

S0006-2960(98)00597-2 CCC: $15.00
Published on Web 09/05/1998

We recently reported that the sulfhydryl-modifying reagent *N*-ethylmaleimide (NEM) inactivates Ssa1p by reacting with its three cysteine residues, which are located in the nucleotide-binding domain (*30*). NEM-modified cysteine residues may interfere with the binding of substrates and their metal ion ligands or disrupt the conformation of Ssa1p. In the experiments described herein, we demonstrate using size exclusion chromatography, circular dichroism, 1-anilinonaphthalene-8-sulfonic acid (ANS) fluorescence, intrinsic tryptophan fluorescence, and limited proteolysis that NEM alters Ssa1p's oligomeric structure and the conformations of its nucleotide- and polypeptide-binding domains. Although NEM inhibits the ATP−agarose binding, ATPase, and protein translocation activities of Ssa1p (*30*), nucleotides and polypeptides bind to NEM-modified Ssa1p (NEM-Ssa1p) and its domains remain coupled. Nucleotide-dependent changes in the intrinsic fluorescence of Ssa1p's only tryptophan residue located in the α-helical lid covering the peptide binding cleft are consistent with a model in which the lid is open in the presence of ATP, but closed in the presence of ADP.

EXPERIMENTAL PROCEDURES

Proteins and Polypeptides. Ssa1p was purified from *S. cerevisiae* MW141 using ATP affinity chromatography and DEAE-cellulose chromatography (*31*). Purified Ssa1p was rendered nucleotide-free by dialyzing it for 48 h at 4 °C against 20 mM HEPES (pH 7.4), 50 mM KCl, 0.1 mM dithiothreitol (DTT), and 0.1 mM EDTA (*22*). Protein concentrations were determined using the method of Bradford (*32*), and bovine γ globulin (Bio-Rad) was used as the standard. The preparation and use of Pep70 (GLQLSLT) were described previously (*22*).

NEM Inactivation of Ssa1p. Nucleotide-free Ssa1p (0.425 mL, 11 mg/mL) was treated with or without 10 mM NEM (*30*) in a final volume of 0.5 mL for 15 min at 20 °C. The samples were then incubated with a final concentration of 20 mM DTT for 10 min at 4 °C, and the resulting mixtures were dialyzed overnight at 4 °C against 20 mM HEPES (pH 7.4), 50 mM KCl, and 0.1 mM DTT. We have previously demonstrated that 3.6 mol of [^{14}C]NEM can be incorporated per mole of nucleotide-free Ssa1p (*30*). Of these, 3.2 mol was distributed among Ssa1p's three cysteine residues, whereas 0.4 mol was distributed among at least 12 other amino acid residues (*30*).

Size Exclusion Chromatography. Ssa1p and NEM-Ssa1p (0.7 mg/mL) were incubated in 0.22 mL of 20 mM HEPES, 50 mM KCl, 2 mM $MgCl_2$, and 0.1 mM DTT containing different combinations of nucleotides and Pep70 for 30 min at 25 °C. Samples (200 μL) were then injected at 4 °C into an FPLC system (Pharmacia Biotech, Inc.) equipped with a Superdex 200 column equilibrated with the same buffer containing either no nucleotides, 1 mM MgADP, or 1 mM MgATP. Proteins were eluted at 0.5 mL/min, and the amount of protein in column fractions (0.5 mL) was quantified (*32*).

Nondenaturing PAGE. Ssa1p or NEM-Ssa1p (0.31 mg/mL) was incubated in 20 μL of 20 mM HEPES (pH 7.4), 50 mM KCl, 2 mM $MgCl_2$, and 2 mM DTT containing different combinations of nucleotides and Pep70 for 30 min at 25 °C. After 5 μL of 5× electrophoresis sample buffer was added, samples were applied to 5% nondenaturing polyacrylamide gels and electrophoresed at 4 °C as previously described (*33*). Buffers for the separating gel and the upper and lower chambers (*33*) contained either no nucleotides, 1 mM MgADP, or 1 mM MgATP. Proteins were detected using Coomassie Blue (*34*).

SDS−PAGE. Ssa1p, NEM-Ssa1p, and their tryptic fragments were separated on 10% SDS−PAGE gels as described by Laemmli (*35*). The protein standards (Sigma) used were phosphorylase *b* (97.4 kDa), bovine serum albumin (66.2 kDa), carbonic anhydrase (45 kDa), ovalbumin (32 kDa), soybean trypsin inhibitor (21.5 kDa), and lysozyme (14.4 kDa). The relative amounts of polypeptides on polyacrylamide gels were quantified using an LKB Ultroscan-XL Enhanced Laser Densitometer.

Circular Dichroism. Solutions [9.3 mg/mL protein in 20 mM HEPES (pH 7.4), 50 mM KCl, 0.1 mM EDTA, and 0.1 mM DTT] of purified nucleotide-free Ssa1p and NEM-Ssa1p were diluted 30-fold to a volume of 300 μL to give a final concentration of 0.31 mg/mL. The far-UV circular dichroism spectra of the Ssa1p and NEM-Ssa1p with, and without nucleotides (MgATP or MgADP), were measured with an Aviv Associates (Lakewood, NJ) model 60DS CD spectrometer using a 0.1 cm path length quartz cell at 25 °C. Nucleotides, when present, were added to a concentration of 50 μM with 1 mM $MgCl_2$. The thermal denaturation of Ssa1p and NEM-Ssa1p, in the presence and absence of ADP, was followed by circular dichroism. The ellipticity at 222 nm was averaged over a 30 s time period every 150 s as the temperature was increased at a constant rate of 0.33 °C/min from 4 to 90 °C. ADP, when present in thermal denaturation reaction mixtures, was added to a concentration of 1 mM (5 mM $MgCl_2$).

ANS and Intrinsic Fluorescence. Ssa1p and NEM-Ssa1p (0.5 mg/mL) were incubated for 30 min in 300 μL of 20 mM HEPES, 50 mM KCl, 2 mM $MgCl_2$, and 0.1 mM DTT containing different combinations of nucleotides and Pep70. For intrinsic fluorescence measurements, samples were excited at 295 nm and emission spectra were recorded from 300 to 450 nm. For ANS fluorescence measurements, samples were incubated with 100 uM ANS (Molecular Probes) at room temperature for 3 h. Then, samples were excited at 380 nm and ANS emission spectra recorded from 420 to 600 nm. Spectra were recorded at room temperature using a model LS5B Perkin-Elmer luminescence spectrophotometer. Excitation and emission slit widths were 3 and 10 nm, respectively. Spectra of samples lacking Ssa1p and NEM-Ssa1p were subtracted from reported spectra.

Trypsin Digestions. Ssa1p and NEM-Ssa1p (0.33 mg/mL) were digested with trypsin (sequencing grade, Boehringer Mannheim) at 25 °C in 20 mM HEPES (pH 7.4), 50 mM KCl, 2 mM $MgCl_2$, and 2 mM DTT as previously described (*22*). At the indicated times, 20 μL of the reaction mixtures was mixed with an equal volume of 2× sample buffer (*22*) and the mixture boiled for 2 min and then applied to SDS−PAGE gels. To more clearly display the array of tryptic fragments generated from NEM-Ssa1p, we used 10% gels in this study instead of 12% gels which were used previously (*22*).

Western Blotting. Tryptic fragments of Ssa1p and NEM-Ssa1p were transferred to nitrocellulose and probed with an

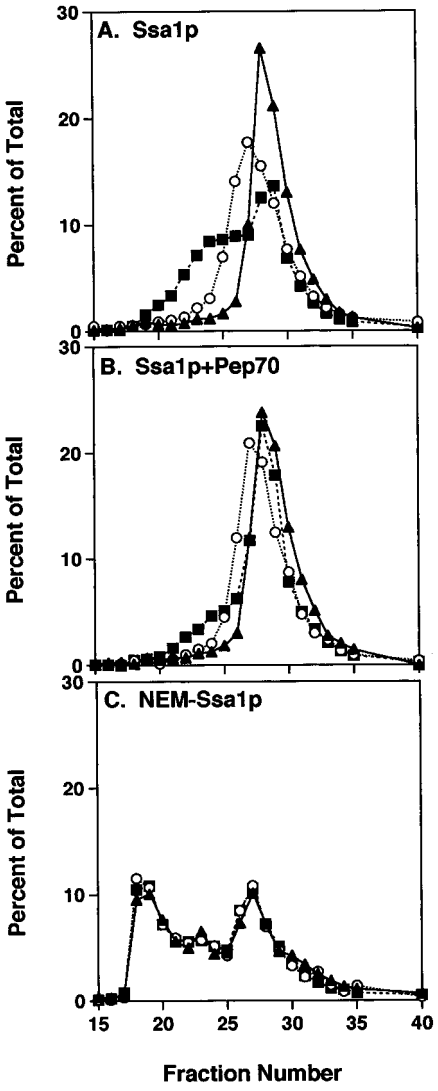

FIGURE 1: Changes in the distribution of monomers, dimers, and oligomers in Ssa1p and NEM-Ssa1p. Ssa1p (A and B) and NEM-Ssa1p (C) were incubated with (B) or without (A and C) Pep70 and either no nucleotides (○), MgADP (■), or MgATP (▲) and then separated on a size exclusion column as described in Experimental Procedures. The amount of protein in each fraction is reported as a percentage of the total recovered. Fractions 15−21, 22−24, and 25−35 contained oligomers, dimers, and monomers, respectively.

antibody specific for the C terminus of Ssa1p (1:1000, anti-Ssa1c antibody) as previously described (*22*).

RESULTS

NEM Alters the Oligomeric Structure of Ssa1p. Hsp70 molecular chaperones exist as monomers, dimers, and larger oligomers (*13*−*17*). The relative amounts of these forms are influenced by nucleotides and polypeptide substrates (*13*−*17*). To determine whether NEM alters the oligomeric structure of Ssa1p, we compared the migrations of Ssap1 and NEM-Ssa1p in the presence of different combinations of ATP, ADP, and Pep70 during size exclusion chromatography and nondenaturing PAGE. In the presence of ATP, Ssa1p migrated primarily as a monomer during size exclusion chromatography (93%, Figure 1A). In the presence of ADP, Ssa1p was distributed among monomers (70%), dimers (21%), and larger oligomers (8%). Peak assignments were confirmed by cross-linking proteins in column fractions using glutaraldehyde and analyzing the products using SDS−PAGE (data not shown). Nucleotide-free Ssa1p was primarily monomeric and migrated slightly faster than the monomeric forms of nucleotide-bound Ssa1p (Figure 1A). Pep70 did not markedly alter the distribution of Ssa1p forms in the absence of nucleotides or in the presence of ATP (compare panels A and B of Figure 1). However, in the presence of ADP, Pep70 increased the amount of monomers by 14% and decreased the amount of dimers and larger oligomers by 10 and 4%, respectively. These results indicate that either ATP or ADP and Pep70 together favor the formation of Ssa1p monomers. These findings agree with those reported by other groups working with Ssa1p (*13*) or other Hsp70s (*13*, *14*, *16*, *17*, *36*).

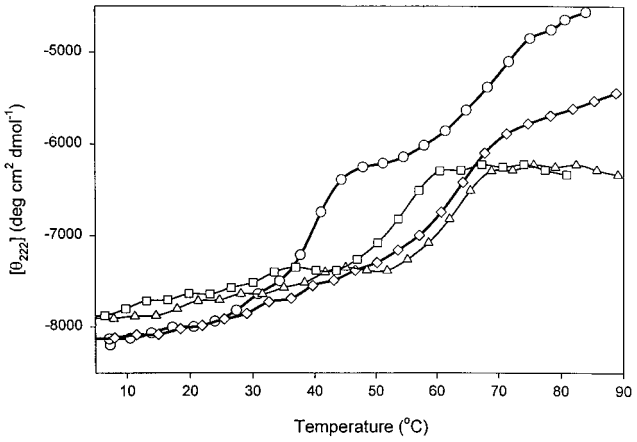

FIGURE 2: Thermal unfolding of Ssa1p and NEM-Ssa1p. The thermal denaturation of Ssa1p (○), Ssa1p with ADP (□), NEM-Ssa1p (◇), and NEM-Ssa1p with ADP (△) was monitored by circular dichroism at 222 nm.

The distribution of NEM-Ssa1p oligomers was very different from that of Ssa1p. In the absence of nucleotides or in the presence of ADP or ATP, NEM-Ssa1p (Figure 1C) was distributed among large oligomers (35%), dimers (16%), and monomers (47%). NEM-Ssa1p monomers and dimers migrated slightly faster than the corresponding forms of Ssa1p. Essentially identical patterns were obtained in the presence of Pep70 (data not shown). Large oligomers were distributed into monomers, dimers, and oligomers during rechromatography, indicating that the various forms of NEM-Ssa1p are in equilibrium (data not shown). Together, these results indicate that NEM alters the oligomeric structure of Ssa1p. Furthermore, nucleotide and polypeptide substrates are less able to depolymerize oligomers of NEM-Ssa1p than those of Ssa1p. Similar results were obtained using nondenaturing PAGE (data not shown).

Circular Dichroism. We have previously shown that the thermal stability of Hsp70s is very sensitive to the presence of nucleotides, and that thermal denaturation is a multiphasic process (*17*, *28*). To ascertain the effects of the NEM modification on the stability of Ssa1p, we followed the denaturation of the modified and unmodified proteins using far-UV circular dichroism. As can be seen from Figure 2, the initial transition occurs at 41 °C in the unmodified Ssa1p, but is shifted to ∼60 °C upon NEM modification. Such a major change in stability has been observed previously when ADP or ATP was bound to Hsp70s (*17*, *28*). With Hsc70 and DnaK, the midpoint of the initial transition in the

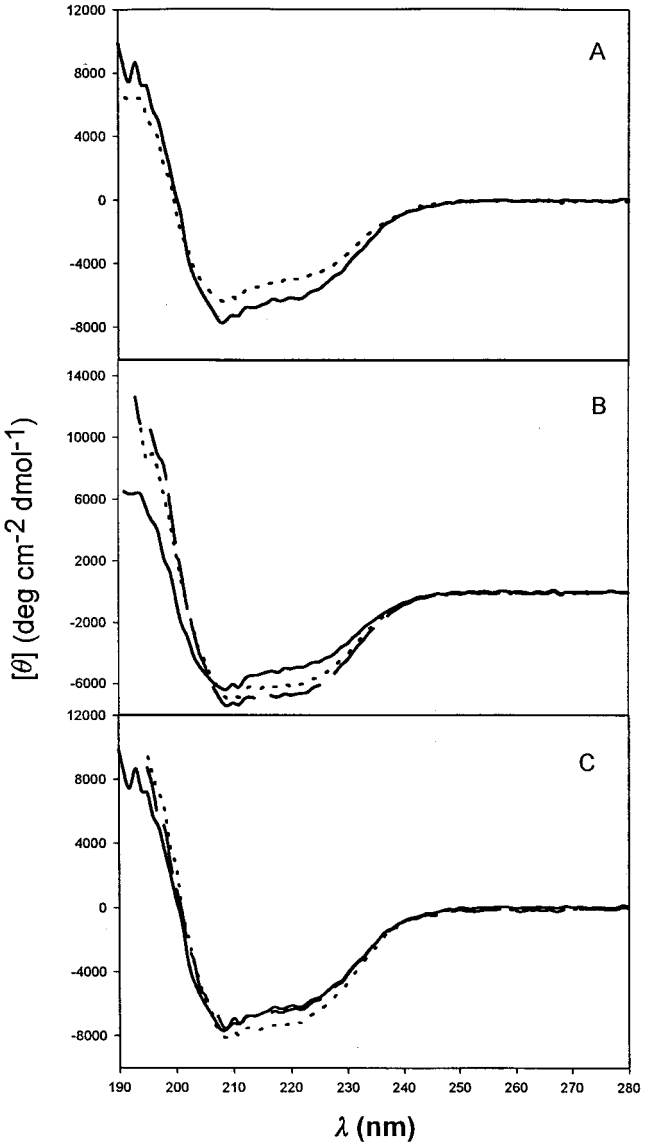

FIGURE 3: Circular dichroism (CD) of Ssa1p and NEM-Ssa1p with and without nucleotides. The CD was measured at 25 °C in a 0.1 cm path length quartz cell. All protein concentrations were 0.31 mg/mL. (A) Far-UV CD of Ssa1p (dotted line) and NEM-Ssa1p (solid line). (B) Far-UV CD of Ssa1p (solid line), Ssa1p with 50 μM ATP/1 mM $MgCl_2$ (dotted line), and Ssa1p with 50 μM ADP/1 mM $MgCl_2$ (dashed line). (C) Far-UV CD of NEM-Ssa1p (solid line), NEM-Ssa1p with 50 μM ATP/1 mM $MgCl_2$ (dotted line), and NEM-Ssa1p with 50 μM ADP/1 mM $MgCl_2$ (dashed line).

presence of ADP is 57−60 °C, the same as for the modified Ssa1p. Therefore, examining the effects of the presence of ADP on the denaturation transitions was of interest. As shown in Figure 2, 1 mM MgADP shifts the midpoint of the initial transition for the unmodified protein to >50 °C, but has only a small effect on the NEM derivative. The curves shown are at equilibrium, and are reversible, indicating that negligible irreversible denaturation occurs (data not shown). These observations suggest that NEM modification has an effect on stability similar to that of binding of ADP.

Comparison of the far-UV CD spectra (Figure 3A) suggests that there are small but significant differences between Ssa1p and NEM-Ssa1p. Since the far-UV CD signal reflects the secondary structure of the protein, these observations suggest that there are small changes in the secondary structure induced by NEM labeling. A difference

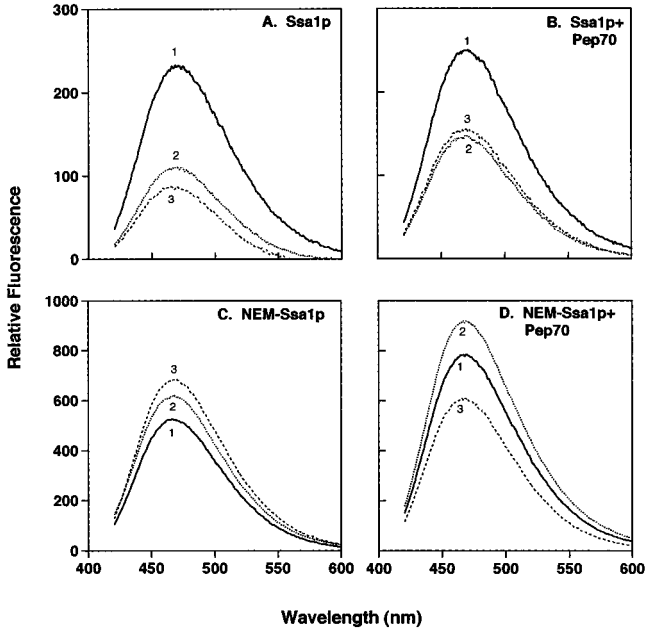

FIGURE 4: ANS fluorescence reveals different conformations of Ssa1p and NEM-Ssa1p. Ssa1p (A and B) or NEM-Ssa1p (C and D) was incubated with (B and D) or without (A and C) Pep70 and either no nucleotides (curve 1), MgADP (curve 2), or MgATP (curve 3), and then their ANS emission spectra were recorded as described in Experimental Procedures. Note that the scale used in panels C and D is greater than that in panels A and B.

spectrum between the modified and unmodified protein revealed that the difference corresponded to a change in the amount of α-helix. In the presence of MgATP, Ssa1p (Figure 3B) and NEM-Ssa1p (Figure 3C) both showed a similar amount of increased ellipticity (negative), relative to the nucleotide-free chaperone. Interestingly, in the presence of MgADP, Ssa1p (Figure 3B) showed a significant increase in (negative) ellipticity, whereas NEM-Ssa1p (Figure 3C) showed no change. These observations indicate that binding of nucleotides may have a small effect on the secondary structure of Ssa1p. Changes were also observed when the peptide was added to Ssa1p but are difficult to interpret unambiguously, since the observed small changes may reflect conformational changes in the peptide and/or the chaperone (data not shown).

NEM Exposes Hydrophobic Surfaces of Ssa1p. We used ANS fluorescence to determine whether the conformation of NEM-Ssa1p, like that of Ssa1p, changes in response to nucleotides and polypeptides. ANS fluorescence increases upon binding hydrophobic surfaces (*37*). In the absence of nucleotides, ANS fluorescence of NEM-Ssa1p (Figure 4C, curve 1) was 2.3-fold greater than that of Ssa1p (Figure 4A, curve 1). The λ_{max} of NEM-Ssa1p was 466 nm, whereas that of Ssa1p was 471 nm. Pep70 further enhanced the ANS fluorescence of Ssa1p (Figure 4A,B, curve 1) and NEM-Ssa1p (Figure 4C,D, curve 1) by 8 and 49%, respectively. Together, these results indicate that the conformations of the nucleotide-free forms of Ssa1p and NEM-Ssa1p are different. They suggest that NEM modification exposes some hydrophobic areas of Ssa1p and that Pep70 alters the conformations of both proteins.

In the presence of ADP, ANS fluorescence of NEM-Ssa1p (Figure 4C, curve 2) was 5.6-fold greater than that of Ssa1p (Figure 4A, curve 2), suggesting that the ADP-bound form

of NEM-Ssa1p has more hydrophobic surfaces exposed than that of Ssa1p. The ANS fluorescence of the ADP-bound form of Ssa1p was 48% less (Figure 4A, curves 1 and 2) whereas that of NEM-Ssa1p was 20% more (Figure 4C, curves 1 and 2) than those of their corresponding nucleotide-free forms. These results suggest that upon binding ADP some hydrophobic surfaces are shielded in Ssa1p, but exposed in NEM-Ssa1p. Pep70 enhanced ANS fluorescence of the ADP-bound forms of Ssa1p (Figure 4A,B, curve 2) and NEM-Ssa1p (Figure 4C,D, curve 2) by 33 and 48%, respectively. These results suggest that Pep70 alters the conformation of the ADP-bound forms of both proteins.

Similar to the effect of ADP on ANS fluorescence, the fluorescence of the ATP-bound form of NEM-Ssa1p (Figure 4C, curve 3) was 7.9-fold greater than that of Ssa1p (Figure 4A, curve 3), suggesting that their ATP-dependent conformations are different from each other. Like the ADP effects described above, ATP quenched the ANS fluorescence of nucleotide-free Ssa1p by 62% (Figure 4A, curves 1 and 3), whereas ATP enhanced that of nucleotide-free NEM-Ssa1p by 31% (Figure 4C, curves 1 and 3). These results suggest that both Ssa1p and NEM-Ssa1p adopt ATP-dependent conformations. Some hydrophobic regions may be shielded in Ssa1p but exposed in NEM-Ssa1p upon binding ATP. Pep70 enhanced the ANS fluorescence of the ATP-bound form of Ssa1p by 1.8-fold (Figure 4A,B, curve 3) but quenched that of NEM-Ssa1p by 12% (Figure 4C,D, curve 3). Thus, in the presence of ATP, some hydrophobic regions may be exposed in Ssa1p but shielded in NEM-Ssa1p upon binding Pep70.

Nucleotide- and Polypeptide-Binding Domains of Ssa1p Remain Coupled after NEM Modification. Ssa1p contains one tryptophan residue (Trp575), which is located in its polypeptide-binding domain. To determine whether NEM modification affects the environment of Trp575 and the coupling of the nucleotide- and polypeptide-binding domains, we measured the intrinsic fluorescence of Ssa1p and NEM-Ssa1p in the presence of different combinations of nucleotides and Pep70 (Figure 5). Because Pep70 lacks tryptophan, changes in intrinsic fluorescence reflect conformational changes of Ssa1p and NEM-Ssa1p. In the absence of nucleotides, the intrinsic fluorescence of NEM-Ssa1p was 1.3-fold greater than that of Ssa1p (Figure 5A,C, curve 1). The λ_{max} of NEM-Ssa1p was 337 nm, whereas that of Ssa1p was 341 nm. These results suggest that the environment of Trp575 in NEM-Ssa1p is more hydrophobic than that in Ssa1p. Pep70 altered the intrinsic fluorescence of nucleotide-free Ssa1p (Figure 5A,B, curve 1) and NEM-Ssa1p (Figure 5C,D, curve 1) by less than 5%, suggesting that it does not markedly perturb the environment of Trp575.

In the presence of ADP, the intrinsic fluorescent spectra of Ssa1p and NEM-Ssa1p were essentially identical to each other, indicating that their Trp575 environments are similar (Figure 5A,C, curve 2). ADP increased the intrinsic fluorescence of nucleotide-free Ssa1p by 16% (Figure 5A, curves 1 and 2), whereas it quenched that of NEM-Ssa1p by 11% (Figure 5C, curves 1 and 2). In the presence of ADP, Pep70 quenched the fluorescence of Ssa1p by 7% (Figure 5A,B, curve 2) and that of NEM-Ssa1p by 24% (Figure 5C,D, curve 2). Thus, binding of Pep70 leads to greater exposure of Trp575 to solvent in both proteins. These results further support the conclusion that NEM-Ssa1p can bind nucleotides and polypeptides. They also suggest that the nucleotide- and polypeptide-binding domains of Ssa1p remain coupled after NEM modification.

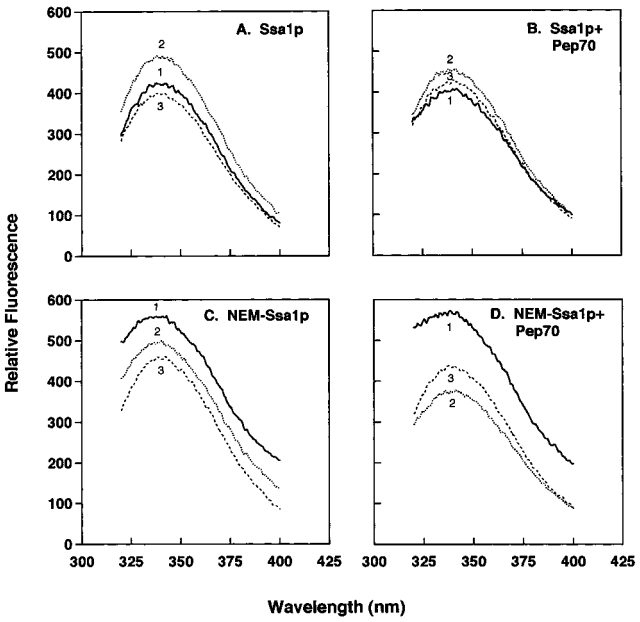

FIGURE 5: Coupling of nucleotide- and polypeptide-binding domains of Ssa1p and NEM-Ssa1p revealed by intrinsic fluorescence. Ssa1p (A and B) or NEM-Ssa1p (C and D) was incubated with (B and D) or without (A and C) Pep70 and either no nucleotides (curve 1), MgADP (curve 2), or MgATP (curve 3), and then their intrinsic fluorescence spectra were recorded as described in Experimental Procedures.

The intrinsic fluorescence of the ATP-bound form of NEM-Ssa1p was 1.2-fold greater than that of Ssa1p (Figure 5A,C, curve 3). This suggests that the environment of Trp575 in NEM-Ssa1p is more hydrophobic than that of Ssa1p. ATP quenched the intrinsic fluorescence of the nucleotide-free form of Ssa1p by 6% (Figure 5A, curves 1 and 3) and that of NEM-Ssa1p by 18% (Figure 5B, curves 1 and 3). Pep70 enhanced the intrinsic fluorescence of the ATP form of Ssa1p by 8% (Figure 5A,B, curve 3) but decreased that of NEM-Ssa1p by 5% (Figure 5C,D, curve 3), resulting in essentially identical spectra (Figure 5B,D, curve 3). Together, these results indicate that Ssa1p and NEM-Ssa1p adopt nucleotide-specific conformations. Because Trp575 is located in the polypeptide-binding domain and its intrinsic fluorescence is affected by nucleotides, they support the conclusion that the nucleotide- and polypeptide-binding domains of Ssa1p remain coupled after NEM modification.

NEM Disrupts the Structure of the Nucleotide-Binding Domain of Ssa1p. To further characterize the effect of NEM on the structure and interdomain coupling of Ssa1p, we probed the structures of Ssa1p and NEM-Ssa1p with trypsin in the presence of different combinations of ADP, ATP, and Pep70. We previously used this method to reveal nucleotide- and polypeptide-dependent conformational changes of Ssa1p (*22*). In the presence of ADP and the absence of Pep70, we determined that NEM-Ssa1p was degraded 18-fold faster than Ssa1p by trypsin, suggesting that their conformations are different (Figure 6A). NEM-Ssa1p was also rapidly degraded in the absence of nucleotides or in the presence of different combinations of ATP and Pep70 (data not shown). These results suggest that trypsin-sensitive sites may be more

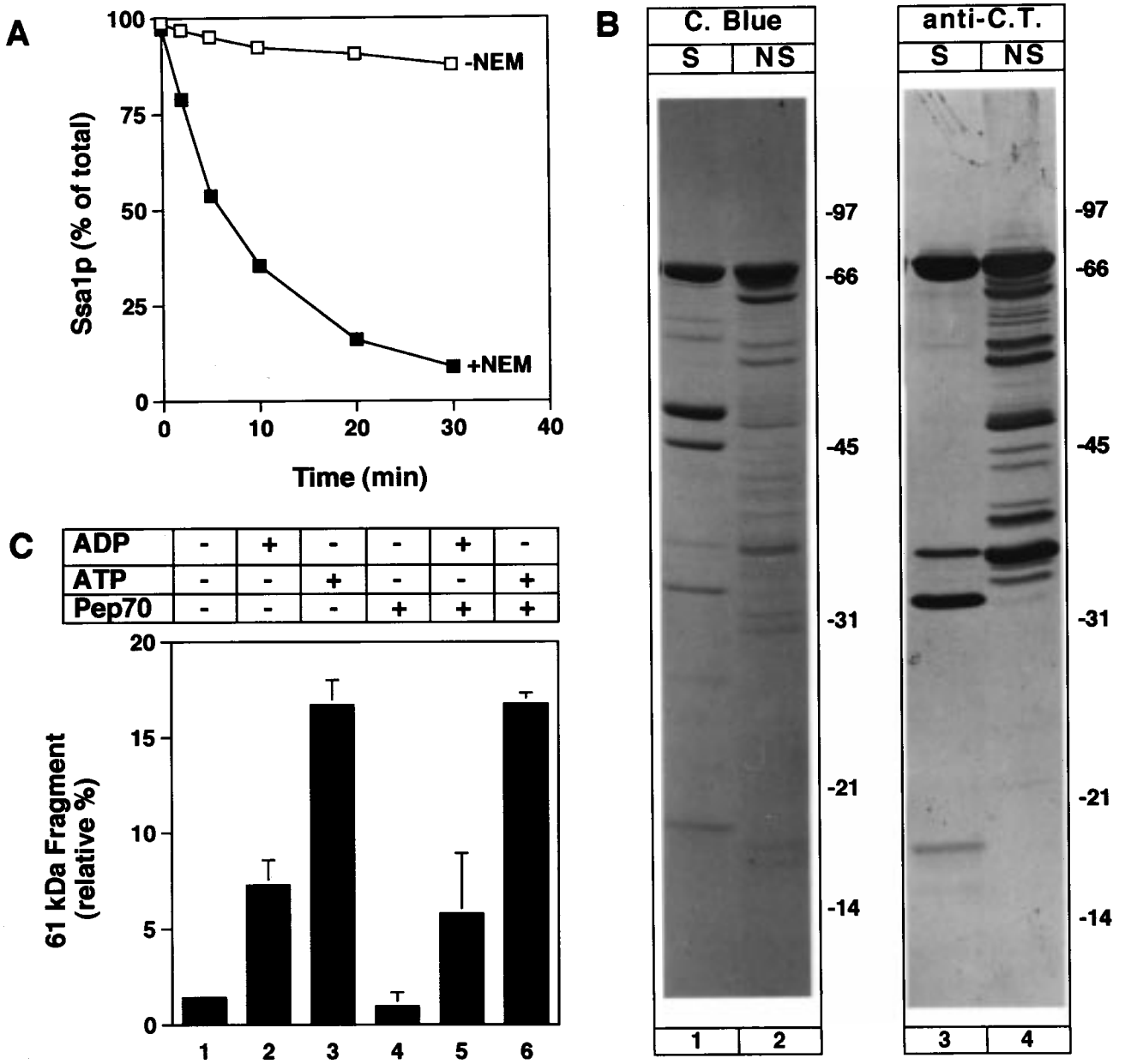

FIGURE 6: Increased trypsin sensitivity of the nucleotide-binding domain of Ssa1p after NEM modification. (A) Time course of trypsin digestion. Ssa1p (310 μg/mL, −NEM) and NEM-Ssa1p (310 μg/mL, +NEM) were incubated with 1 mM MgADP and 0.18 μg/mL of trypsin. At each time point, 20 μL was removed and immediately mixed with SDS−PAGE sample buffer and boiled. Tryptic fragments were separated on SDS−PAGE gels and quantified as described in Experimental Procedures. The values reported are the average of two determinations. (B) Identification of tryptic fragments. In the presence of 1 mM MgATP, Ssa1p (310 μg/mL, S) was digested with trypsin (34 μg/mL) for 40 min (lanes 1 and 3) and NEM-Ssa1p (310 μg/mL, NS) was digested with trypsin (0.28 μg/mL) for 10 min (lanes 2 and 4). Fragments were then separated on SDS−PAGE gels and then either stained with Coomassie Blue (C. Blue, lanes 1 and 2) or transferred to nitrocellulose and probed with an antibody that recognizes the carboxyl terminus of Ssa1p (anti-C. T., lanes 3 and 4). Numbers at the right indicate the molecular masses and migrations of standards. (C) Quantification of nucleotide-sensitive 61 kDa fragment of NEM-Ssa1p. NEM-Ssa1p (0.31 mg/mL) was incubated with (lanes 4−6) or without (lanes 1−3) Pep70 and either no nucleotides (lanes 1 and 4), 1 mM MgADP (lanes 2 and 5), or 1 mM MgATP (lanes 3 and 6) and then digested with trypsin (0.55 μg/mL) for 30 min. Fragments were separated on SDS−PAGE gels and stained with Coomassie Blue, and then the relative amount of the 61 kDa fragment in the 50−70 kDa region of the gel was quantified. Values are reported as the means of three separate experiments ± standard deviation.

accessible or that new sites may be exposed after NEM modification.

To determine whether NEM exposes new trypsin-sensitive sites, we digested NEM-Ssa1p and Ssa1p to about 75% completion and then separated the fragments on SDS−PAGE gels. Ssa1p was digested into about seven fragments, whereas NEM-Ssa1p was digested into at least 25 fragments (Figure 6B, lanes 1 and 2). These results indicate that NEM modification of Ssa1p exposes new trypsin-sensitive sites.

Using an antibody that recognizes the C terminus of Ssa1p (*22*), we probed Western blots of Ssa1p and NEM-Ssa1p tryptic fragments to determine whether they are derived from the polypeptide-binding domain. The antibody recognized three (36, 32, and 19 kDa) of the seven fragments of Ssa1p as previously reported (Figure 6B, lane 3). In contrast, at least 15 fragments of NEM-Ssa1p ranging is size from 32 to 64 kDa were recognized by the antibody (Figure 6B, lane 4). Because the polypeptide-binding domain of Hsp70s is

about 27 kDa, tryptic fragments which are recognized by this antibody and which are larger than 27 kDa are derived from trypsin-sensitive sites located in the nucleotide-binding domain. The 36 kDa fragment in both Ssa1p and NEM-Ssa1p digests was recognized by the antibody (Figure 6B, lanes 3 and 4). Thus, NEM modification exposed at least 14 new trypsin-sensitive sites in the 44 kDa nucleotide-binding domain of Ssa1p.

The intrinsic fluorescence experiments described above revealed that the binding of nucleotides affects the conformation of the polypeptide-binding domain of Ssa1p and NEM-Ssa1p. To further investigate the effect of NEM on interdomain communication in Ssa1p, we incubated nucleotide-free NEM-Ssa1p with different combinations of nucleotides and Pep70, treated the samples with trypsin, separated the fragments on SDS−PAGE gels, and quantified the fragments using laser densitometry. Of the 20 tryptic fragments detected after about 90% digestion of NEM-Ssa1p, only the amount of a 61 kDa fragment changed in response to nucleotides. The amounts of the 61 kDa fragment in the presence of ADP and ATP were 3.8- and 8.8-fold, respectively, greater than those in the absence of nucleotides (Figure 6C). We did not detect Pep70-dependent changes in the 61 kDa fragment (Figure 6C) or other tryptic fragments (data not shown). The 61 kDa fragment was not recognized by the antibody specific for the C terminus (data not shown), indicating that it is derived from at least one trypsin-sensitive site located in the C-terminal 10 kDa of the polypeptide-binding domain. Together, these results suggest that the nucleotide- and polypeptide-binding domains remain coupled in NEM-Ssa1p.

DISCUSSION

NEM was previously shown to modify Ssa1p's three cysteine residues, which are located in the nucleotide-binding domain, and to inhibit its ATP−agarose binding, ATPase, and protein translocation activities (*30*). We postulated that NEM may either sterically interfere with the binding of nucleotides and their metal ion ligands or alter the conformation of Ssa1p (*30*). In this study, we have shown using size exclusion chromatography, circular dichroism, ANS and intrinsic fluorescence, and limited proteolysis that the conformations of Ssa1p and NEM-Ssa1p are different. We mapped the conformational changes to both the nucleotide- and polypeptide-binding domains. Together, the results demonstrate that conformational changes accompany the NEM-dependent inactivation of Ssa1p. The intrinsic fluorescence experiments also revealed nucleotide- and polypeptide-dependent conformational changes of the α-helical lid covering the polypeptide-binding cleft. To our knowledge, this is the first report of such conformational changes in this region of Hsp70s.

Ssa1p, like other Hsp70s, undergoes nucleotide-dependent oligomerization (*13*−*17*, *19*). Ssa1p monomers predominate in the presence of ATP, whereas a mixture of monomers, dimers, and oligomers are found in the presence of ADP. In contrast, NEM-Ssa1p was found in two main forms: a monomer and a large polymer. Their distribution was not influenced by nucleotides or polypeptide substrates. Benaroudj et al. (*38*) recently found that essentially all of the oligomerization activity of Hsp70s was provided by the polypeptide-binding domain. Furthermore, they showed that a polypeptide substrate converted oligomers of the polypeptide-binding domain to monomers. These results suggested that the polypeptide-binding pocket likely mediates Hsp70 polymerization. In our studies, Pep70 did not depolymerize NEM-Ssa1p, suggesting that a site(s) other than the polypeptide-binding cleft mediates its polymerization.

The effects of NEM modification on the thermal stability of Ssa1p indicate that it significantly increases the stability of Ssa1p. The effect is analogous to that observed by the binding of nucleotides to the unmodified protein. The increase in the size and amount of oligomers upon NEM modification may contribute to the increase in thermal stability.

The circular dichroism spectral changes observed in Ssa1p and its NEM-modified derivative suggest that the presence of the NEM induces a small amount of helix. Since it is possible that the covalently linked NEM itself could contribute a small signal to the far-UV CD spectrum, we cannot be absolutely certain that the observed changes do indeed stem from an NEM-induced change in the secondary structure. However, in light of the conformational changes observed by the other methods used in this study, it is most likely that the presence of the NEM induces an increase in α-helix content. Such an increase may arise from the extension of or decreased "fraying" of existing helices, the conversion of some loop and/or disordered conformation into α-helix, or an overall increase in the rigidity of the molecule leading to general tightening up of the helices. The differences noted between the effects of ADP and ATP binding on secondary structure also reveal differences in the effects of nucleotide binding on the conformation of the chaperone.

NEM may alter the conformation of Ssa1p by sterically disrupting the local environment of the modified cysteine residues. Cys15 is located at the base of the nucleotide-binding pocket in subdomain IA in a β-strand that interacts with the α- and β-phosphates of ADP and their metal ion ligands (*39*, *40*). Cys264 and Cys303 are located in subdomain IIB. Cys264 is located in an α-helix that lines one side of the nucleotide-binding pocket, whereas Cys303 is located in an α-helix on the outer surface of Ssa1p. NEM-Ssa1p migrates slightly faster during size exclusion chromatography and has more trypsin-sensitive sites than Ssa1p, suggesting that it is less tightly packed than Ssa1p. The nucleotide- and polypeptide-dependent forms of NEM-Ssa1p examined in this study had greater ANS fluorescence than the corresponding forms of Ssa1p. ANS fluorescence may increase because it is in a more hydrophobic environment, more of it is bound in hydrophobic environments, or its binding is tighter. Since ANS has an affinity for nucleotide-binding pockets (*27*), the greater ANS fluorescence may also indicate that the nucleotide-binding pocket of NEM-Ssa1p may be more accessible to this fluorescent probe. NEM-Ssa1p's conformationally changed nucleotide-binding domain and exposed hydrophobic surfaces may contribute to its polymerization. ANS may also bind at the interfaces of adjacent Ssa1ps in oligomers. Although the location of the new trypsin-sensitive sites in NEM-Ssa1p suggests that the conformational changes are restricted to the nucleotide-binding domain, the intrinsic fluorescence studies indicated

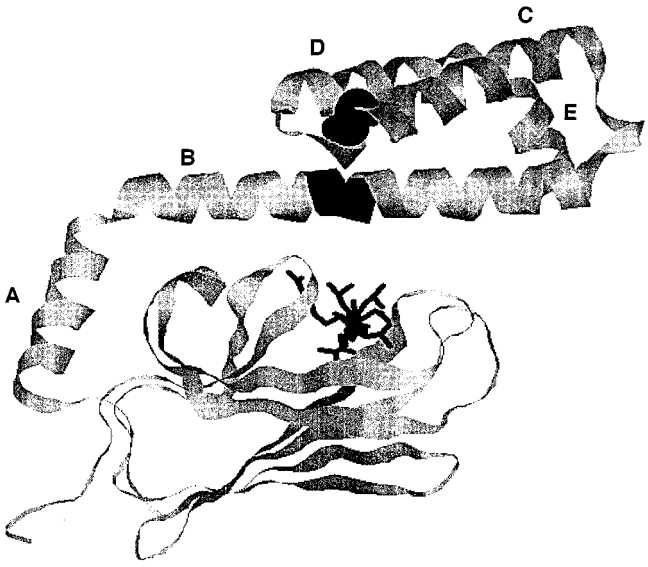

FIGURE 7: Location of Ssa1p's Trp575 based on the three-dimensional structure of the polypeptide-binding domain of DnaK. The position of Ssa1p's Trp575 (Ala575 in DnaK) is indicated by the space-filled group. The stick structure represents a polypeptide bound in the β-sandwich. The origin of the kink (residues 536−538 of DnaK) that may allow the α-helical lid to open and close is indicated by the black ribbon. α-Helices A−E are labeled. The figure was constructed using the coordinates of the polypeptide-binding domain of DnaK (*41*) and RasMol, version 2.5.

that some changes are also associated with the polypeptide-binding domain. NEM-Ssa1p's conformation may also include a misalignment of the nucleotide- and polypeptide-binding domains.

Solution small-angle X-ray-scattering analysis of Hsc70 (*24*) led to a model in which its nucleotide- and polypeptide-binding domains are packed together in the presence of ATP but more loosely associated in the presence of ADP. Our results showing that the ATP-bound form of Ssa1p has the lowest ANS fluorescence are consistent with this form being the most tightly packed. In the presence of ADP, more hydrophobic surfaces may be exposed. Perhaps one of these surfaces mediates interactions between the nucleotide- and polypeptide-binding domains in the ATP state.

Changes in the intrinsic fluorescence of Ssa1p's single tryptophan residue, which is located in the polypeptide-binding domain, provided new information about the nucleotide- and polypeptide-dependent conformational changes of this region. The polypeptide-binding domain of DnaK (Figure 7) is composed of a β-sandwich and five α-helices (*41*). The β-sandwich has two sheets each containing four β-strands. Two loops rise above the plane of the upper sheet and form the polypeptide-binding cleft. Zhu et al. (*41*) have suggested that the five α-helices (A−E) act as a lid covering the cleft that must be displaced to facilitate polypeptide binding. Of these, α-helix B is closest to bound polypeptide, but does not directly contact it. A comparison of two crystal forms of the polypeptide-binding domain of DnaK suggested that a kink originates near residues 536−538 (Figure 7, black ribbon) of helix B, allowing the α-helical lid to open (*41*). The lack of peptide-binding activity of Hsc70 mutants containing deletions in either α-helix A or C suggests that they play an important role in the structure or function of the α-helical lid (*42*). On the basis of the three-dimensional structure of DnaK, Ssa1p's Trp575 (Figure 7, space-filled group) is located in α-helix C near the origin of the kink and forms part of the hydrophobic core of the lid. Trp575 is conserved in several Hsp70s, including bovine Hsc70 and human Hsp70, but not in DnaK where an alanine residue occupies this site. Because the nucleotide- and polypeptide-binding domains of bovine Hsc70 and human Hsp70 each contain a tryptophan residue, changes in intrinsic fluorescence of these proteins could not be attributed to domain-specific conformational changes (*23*, *25*). We showed above that the intrinsic fluorescence of Trp575 in Ssa1p is quenched in the presence of ATP. The quenching reflects the environment of Trp575 in the ATP-bound form of Ssa1p, which has an open α-helical lid facilitating binding and release of polypeptides. In the presence of ADP, the enhanced intrinsic fluorescence of Trp575 reflects its environment when the α-helical lid is closed, limiting the binding and release of polypeptides. These results provide the first experimental support for the model (*41*) in which the α-helical domain acts as a lid for the polypeptide-binding cleft.

The coupling of the nucleotide- and polypeptide-binding domains regulates the interactions of Hsp70s with nucleotide and polypeptide substrates (*17*, *20*−*26*). Although NEM-Ssa1p lacks ATP−agarose binding, ATPase, and protein translocation activities (*30*), its conformation responds to nucleotides and polypeptides. However, domain coupling is different from that of Ssa1p. The intrinsic fluorescence of Ssa1p with or without Pep70 is greater in the presence of ADP than in the presence of ATP, suggesting that the α-helical lid is closed in the high-affinity state for polypeptides. In contrast, the intrinsic fluorescence of NEM-Ssa1p in the presence of Pep70 and ADP is quenched compared to that of the ATP-bound form, suggesting that the lid is in a more open conformation. Thus, polypeptides may bind more tightly to ATP-bound NEM-Ssa1p than to its ADP-bound form.

ACKNOWLEDGMENT

We thank Dr. Matthew Avitable, Randi Eisen, and Aynih Hermawan for technical assistance, Vincent Garofalo for photography, and Drs. John Lewis and George Ojakian for comments on the manuscript.

REFERENCES

1. Martin, J., and Hartl, F.-U. (1997) *Curr. Opin. Struct. Biol. 7*, 41−52.
2. Landry, S. J., Jordan, R., McMacken, R., and Gierasch, L. M. (1992) *Nature 355*, 455−457.
3. Flynn, G. C., Pohl, J., Flocco, M. T., and Rothman, J. E. (1991) *Nature 353*, 726−730.
4. Blond-Elguindi, S., Cwirla, S. E., Dower, W. J., Lipshutz, R. J., Sprang, S. R., Sambrook, J. F., and Gething, M. J. (1993) *Cell 75*, 717−728.
5. Rudiger, S., Buchberger, A., and Bukau, B. (1997) *Nat. Struct. Biol. 4*, 342−349.
6. Langer, T., Lu, C., Echols, H., Flanagan, J., Hayer, M. K., and Hartl, F.-U. (1992) *Nature 356*, 683−689.
7. Szabo, A., Langer, T., Schröder, H., Flanagan, J., Bukau, B., and Hartl, F.-U. (1994) *Proc. Natl. Acad. Sci. U.S.A. 91*, 10345−10349.
8. Flynn, G. C., Chappell, T. G., and Rothman, J. E. (1989) *Science 245*, 385−390.
9. Palleros, D. R., Reid, K. L., Shi, L., Welch, W. J., and Fink, A. L. (1993) *Nature 365*, 664−666.

10. Schmid, D., Baici, A., Gehring, H., and Christen, P. (1994) *Science 263*, 971−973.
11. Liberek, K., Marszalek, J., Ang, D., Georgopoulos, C., and Zylicz, M. (1991) *Proc. Natl. Acad. Sci. U.S.A. 88*, 2874−2878.
12. Cyr, D. M., Lu, X., and Douglas, M. G. (1992) *J. Biol. Chem. 267*, 20927−20931.
13. King, C., Eisenberg, E., and Greene, L. (1995) *J. Biol. Chem. 270*, 22535−22540.
14. Schmid, S. L., Braell, W. A., and Rothman, J. E. (1985) *J. Biol. Chem. 260*, 10057−10062.
15. Wei, J., and Hendershot, L. M. (1995) *J. Biol. Chem. 270*, 26670−26676.
16. Leung, S.-M., Senisterra, G., Ritchie, K. P., Sadis, S. E., Lepock, J. R., and Hightower, L. E. (1996) *Cell Stress Chaperones 1*, 78−89.
17. Palleros, D. R., Welch, W. J., and Fink, A. L. (1991) *Proc. Natl. Acad. Sci. U.S.A. 88*, 5719−5723.
18. Weissbach, H., Redfield, B., Qiu, N., Chen, G., Carlino, A., Vidal, V., Tsolas, O., and Brot, N. (1995) *Cell. Mol. Biol. Res. 41*, 397−403.
19. Blond-Elguindi, S., Fourie, A. M., Sambrook, J. F., and Gething, M. H. (1993) *J. Biol. Chem. 268*, 12730−12735.
20. Buchberger, A., Theyssen, H., Schröder, H., McCarty, J. S., Virgallita, G., Milkereit, P., Reinstein, J., and Bukau, B. (1995) *J. Biol. Chem. 270*, 16903−16910.
21. Kassenbrock, C. K., and Kelly, R. B. (1989) *EMBO J. 8*, 1461−1467.
22. Fung, K. L., Hilgenberg, L., Wang, N. M., and Chirico, W. J. (1996) *J. Biol. Chem. 271*, 21559−21565.
23. Freeman, B. C., Myers, M. P., Schumacher, R., and Morimoto, R. I. (1995) *EMBO J. 14*, 2281−2292.
24. Wilbanks, S. M., Chen, L., Tsuruta, H., Hodgson, K. O., and McKay, D. B. (1995) *Biochemistry 34*, 12095−12106.
25. Ha, J., and McKay, D. B. (1995) *Biochemistry 34*, 11635−11644.
26. Liberek, K., Skowyra, D., Zylicz, M., Johnson, C., and Georgopoulos, C. (1991) *J. Biol. Chem. 266*, 14491−14496.
27. Shi, L., Palleros, D. R., and Fink, A. L. (1994) *Biochemistry 33*, 7536−7546.
28. Palleros, D. R., Reid, K. L., McCarty, J. S., Walker, G. C., and Fink, A. L. (1992) *J. Biol. Chem. 267*, 5279−5285.
29. Morshauser, R. C., Wang, H., Flynn, G. C., and Zuiderweg, E. R. (1995) *Biochemistry 34*, 6261−6266.
30. Liu, Q., Levy, E. J., and Chirico, W. J. (1996) *J. Biol. Chem. 271*, 29937−29944.
31. Brodsky, J. L., Hamamoto, S., Feldheim, D., and Schekman, R. (1993) *J. Cell Biol. 120*, 95−102.
32. Bradford, M. M. (1976) *Anal. Biochem. 72*, 248−254.
33. Lewinsohn, E., Gijzen, M., and Croteau, R. (1992) *Arch. Biochem. Biophys. 293*, 167−173.
34. Waters, M. G., Chirico, W. J., and Blobel, G. (1986) *J. Cell Biol. 103*, 2629−2636.
35. Laemmli, U. K. (1970) *Nature 227*, 680.
36. Wei, J., Gaut, J. R., and Hendershot, L. M. (1995) *J. Biol. Chem. 270*, 26677−26682.
37. Stryer, L. (1965) *J. Mol. Biol. 13*, 482−495.
38. Benaroudj, N., Fouchaq, B., and Ladjimi, M. M. (1997) *J. Biol. Chem. 272*, 8744−8751.
39. Flaherty, K. M., DeLuca-Flaherty, C., and McKay, D. B. (1990) *Nature 346*, 623−628.
40. Wilbanks, S. M., and McKay, D. B. (1995) *J. Biol. Chem. 270*, 2251−2257.
41. Zhu, X., Zhao, X., Burkholder, W. F., Gragerov, A., Ogata, C. M., Gottesman, M. E., and Hendrickson, W. A. (1996) *Science 272*, 1606−1614.
42. Boice, J. A., and Hightower, L. E. (1997) *J. Biol. Chem. 272*, 24825−24831.

BI980597J